

This is the author-accepted manuscript version of the following article: El-Yazbi, A. F.A., & Loppnow, G. R. (2018). Probing DNA Damage Induced by Common Antiviral Agents Using Multiple Analytical Techniques. *Journal of Pharmaceutical and Biomedical Analysis*, 157(2018), 226-234., which has been published in final form at <https://doi.org/10.1016/j.jpba.2018.05.019>

Accepted Manuscript

Title: Probing DNA damage induced by common antiviral agents using multiple analytical techniques

Authors: Amira F. El-Yazbi, Glen R. Loppnow

PII: S0731-7085(18)30149-3
DOI: <https://doi.org/10.1016/j.jpba.2018.05.019>
Reference: PBA 11970

To appear in: *Journal of Pharmaceutical and Biomedical Analysis*

Received date: 17-1-2018
Revised date: 8-5-2018
Accepted date: 15-5-2018

Please cite this article as: Amira F.El-Yazbi, Glen R.Loppnow, Probing DNA damage induced by common antiviral agents using multiple analytical techniques, *Journal of Pharmaceutical and Biomedical Analysis* <https://doi.org/10.1016/j.jpba.2018.05.019>

This is a PDF file of an unedited manuscript that has been accepted for publication. As a service to our customers we are providing this early version of the manuscript. The manuscript will undergo copyediting, typesetting, and review of the resulting proof before it is published in its final form. Please note that during the production process errors may be discovered which could affect the content, and all legal disclaimers that apply to the journal pertain.



Probing DNA damage induced by common antiviral agents using multiple analytical techniques

Amira F. El-Yazbi^{a,b} and Glen R. Lopnow^{a,*}

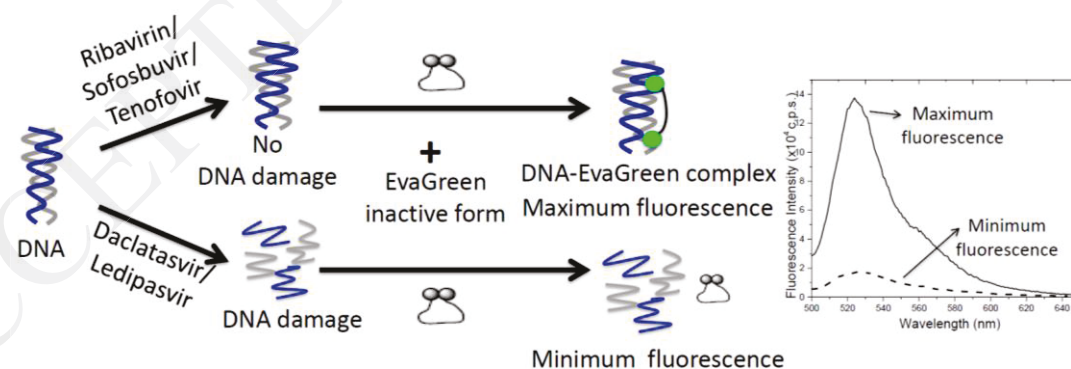
^a Department of Chemistry, University of Alberta, Edmonton, AB T6G 2G2, Canada

^b Department of Pharmaceutical Analytical Chemistry, Faculty of Pharmacy, Alexandria University, Alexandria, Egypt

* Corresponding author. Tel.: (780) 492-9704; Fax: (780) 492-8231.

e-mail address: glen.loppnow@ualberta.ca (G. R. Lopnow).

Graphical abstract



Highlights:

- Absorption spectroscopy, MALDI-TOF mass spectrometry and fluorimetric analysis using an intercalating dye were used to study the DNA damaging effect of five FDA-approved antiviral drugs.
- Two drugs, ledipasvir and daclatasvir, consistently show evidence of drug-induced DNA damage.
- Fluorimetric studies of the rate of the drug-induced DNA damage show its dependence on the drug concentration.
- This work suggests a novel approach for the treatment of hepatitis B and C patients with hepatocellular carcinoma.

Abstract

Hepatocellular carcinoma is one of the most common malignant tumors in the world. Chronic hepatitis B and C infections are the most common etiologies of hepatocellular carcinoma worldwide. In this study, we explore the potential DNA damaging effect of some FDA-approved antiviral drugs which may be able to serve as anticancer agents for hepatocellular carcinoma, in order to better elucidate their mode of action. Five antiviral drugs were selected; ribavirin, sofosbuvir, tenofovir disoproxil fumarate, daclatasvir and ledipasvir. Several methods, including absorption spectroscopy, MALDI-TOF mass spectrometry and fluorimetric analysis using the EvaGreen (EG) intercalating dye, were used to probe the drug-induced DNA damage. Results show that only daclatasvir and ledipasvir induced DNA damage. Absorption spectroscopy showed hyperchromicity in the 280-nm DNA absorption

band of DNA samples incubated with each drug, indicating disruption of the double-strand structure. Mass spectra for DNA samples incubated with each of the two drugs showed a disappearance of the DNA molecular ion peak with a concomitant appearance of peaks with smaller m/z , indicating DNA strand breaks. EG fluorescence was observed to decrease with increasing incubation time of daclatasvir and ledipasvir with DNA, indicating that the EG detaches from the DNA, likely due to DNA damage. All of these results are consistent with DNA damage, proposed as oxidative damage to both nucleobase and deoxyribose moieties of DNA as the mode of action for these two drugs. Moreover, these results are dependent on the antiviral drug concentration and show that DNA regions rich in guanine are affected more than other regions by these two drugs. Therefore, such antiviral drugs may present a promising therapeutic alternative to the currently used anticancer agents, especially for hepatitis B and C patients with hepatocellular carcinoma resistant to conventional treatment approaches.

Keywords

Antiviral agents, Anticancer agents, Hepatocellular carcinoma, DNA damage, Ledipasvir, Daclatasvir, EvaGreen, Absorption spectroscopy, MALDI-TOF mass spectrometry, fluorescence spectroscopy.

1. Introduction

The incidence of hepatocellular carcinoma, the most common type of primary liver cancer, is increasing rapidly [1] with the highest mortality rates being in Asia and Africa [2]. Although several chronic liver diseases are associated with hepatocellular carcinoma, Hepatitis B Virus (HepB) and Hepatitis C Virus (HepC) are statistically the most commonly implicated risk factors [3]. Combined, they are responsible for 85% of total new hepatocellular

carcinoma cases worldwide, 54% occurring as a result of HepB and 31% as a result of HepC [4]. These two viral associations mean that 80% of hepatocellular carcinoma cases are ineligible for curative surgical treatment [5]. Patients with unresectable hepatocellular carcinoma cannot also be cured by systemic chemotherapy or radiotherapy [5] because hepatoma cells respond poorly to these approaches in such cases [6]. Given the limited efficacy of existing treatment for hepatocellular carcinoma associated with HepB and HepC, the development of novel and efficient targeted therapies is required to increase their treatment options, such as the use of antiviral agents to lower the incidence of HepB and HepC.

DNA is one of the primary intracellular targets of anticancer drugs; interaction between small molecules and DNA can cause damage to DNA, blocking cellular division and resulting in cell death [7,8]. Studying the interactions of DNA with drug molecules with different pharmacological actions (e.g. antivirals, antihypertensives, etc.) are important for the identification and design of new efficacious anticancer drugs other than currently used anticancer drugs, such as cis-platin and doxorubicin [9]. Since the development of new anticancer drugs is slow and costly, studying the effect of drugs already approved for indications other than cancer is one possible strategy [10-12]. Small molecules, such as drugs, can interact with DNA via covalent or non-covalent interactions including intercalation, groove binding, or electrostatic attraction [13]. If drug binding causes DNA damage in cancerous cells, then it may affect the replication cycle and may subsequently lead to cell death.

In this study, we will explore the interaction of various antiviral agents with DNA as potential anticancer agents. Ribavirin, sofosbuvir, tenofovir disoproxil fumarate, daclatasvir and ledipasvir are widely used FDA-approved antiviral drugs [14] and therefore we chose

them to investigate their DNA damaging effect. Several spectroscopic techniques have been previously used to detect the interactions of small drug molecules with DNA and to quantitate the damage induced in the DNA, such as UV absorption [11,12,15], fluorescence spectrophotometry using intercalating dyes such as Hoechst 33258 dye [11], ethidium bromide [12,16] and terbium chloride [17], fluorescent molecular beacons [18], circular dichroism spectropolarimetry [11,19], and dynamic viscosity measurements [11,20] Here, we have used several analytical techniques to determine whether DNA is damaged by these antiviral drugs, including mass spectrometry, UV absorption and fluorimetric detection using the EvaGreen intercalating dye [21,22]. The results show that only daclatasvir and ledipasvir induce DNA damage. As a result, daclatasvir and ledipasvir present promising targeted therapies for HepB and/or HepC patients suffering from hepatocellular carcinoma.

2. Experimental

2.1. Materials

Ribavirin (RIB), sofosbuvir (SOF), tenofovir disoproxil fumerate (TEN), ledipasvir (LED) and daclatasvir (DAC) (Table 1) were obtained from Medizen Pharmaceutical Industries Co. (Alexandria, Egypt). All oligonucleotide sequences (Table 2) were obtained from Integrated DNA Technologies Inc. (Coralville, Iowa) and were purified by standard desalting. The calf thymus DNA (ctDNA) was obtained from Sigma-Aldrich Canada Ltd. (Oakville, Ontario). The EvaGreen (EG) dye was obtained from Biotium Inc. (Fremont, California), sodium chloride was obtained from EMD Chemicals Inc. (Gibbstown, New Jersey), Tris was obtained from ICN Biomedicals, (Aurora, Ohio) and ethylenediaminetetraacetic acid (EDTA) was obtained from BDH Inc. (Toronto, Ontario). All

chemicals were used as received. Nanopure water from a Barnsted Nanopure (Boston, Massachusetts) system was used for all solutions. The oligonucleotide solution concentration of 10 μM was prepared in Tris buffer solution (10 mM Tris, 10 mM NaCl, 1 mM EDTA, pH 7.5), gradually heated to 85°C in a water bath and then annealed at room temperature (25°C) in the dark for 24 h before use for all samples.

2.2. Instrumentation

Absorption spectra were recorded on an Agilent 8453 diode array spectrophotometer (San Diego, California). The single fluorescence measurements were performed by using a Photon Technologies International (Birmingham, New Jersey) fluorescence spectrophotometer, while multiplexed fluorescence measurements were performed by using a Safire fluorescence plate reader (Tecan, Mannendorf, Switzerland). For the mass spectrometric analysis, a MALDI-TOF-Mass spec-Elite Voyager (Lancashire, UK) spectrometer equipped with a nitrogen laser was used.

2.3. Procedures

2.3.1. Absorption measurements

For the absorption measurements, 0.5 μM of the random dsDNA sequence (Table 2) was separately mixed with 20 μM of each of the selected antiviral drugs, RIB, TEN, SOF, LED and DAC, in buffer (10 mM Tris, 10 mM NaCl, 1 mM EDTA, pH 7.5). The absorption spectrum of each mixture at incubation times of 0, 6 and 24 hr was recorded to check the progress of the reaction.

2.3.2. MALDI-TOF mass spectrometry

Reaction mixtures of 50 μM of the random dsDNA sequence with 2 mM of each of RIB, TEN, SOF, LED and DAC ([dsDNA]:[drug] = 1:40), were incubated at room temperature for 0, 6 and 24 hr. After incubation, each reaction mixture was loaded onto a sample plate with the matrix 9:1 (2,4,6-trihydroxyacetophenone/diammonium citrate) and measured by a MALDI-TOF-Mass spec-Elite Voyager equipped with a nitrogen laser for ionization and desorption. The nitrogen laser operated at 337 nm with 3 ns pulse delivered to a sample at 20 Hz.

2.3.3. Fluorescence measurements

Only LED and DAC were used in the fluorescence measurements. EG dye was added to the random dsDNA sequence followed by incubation at 37 °C for 20 min in the dark. After an additional 1 hr at room temperature (25°C), LED or DAC was separately added to the dsDNA-EG mixture to reach a final concentration of 0.2 μM dsDNA, 0.3 μM EG and 10 μM LED or DAC in buffer (10 mM Tris, 10 mM NaCl, 1 mM EDTA, pH 7.5). For the control experiments, 10 μM LED or DAC alone was added to 0.3 μM EG in the same buffer (for the drug/EG control), 0.2 μM DNA alone was added to 0.3 μM EG in the same buffer (for the DNA/EG control), 0.3 μM EG alone was prepared in the same buffer (for the EG alone control) or 0.2 μM DNA alone was prepared in the same buffer (for the DNA alone control). Fluorescence spectra of the incubated sample mixtures were measured at three time intervals, 0, 6 and 24 hr, using a Photon Technology International Inc. (Lawrenceville,NJ) fluorimeter. The emission spectra were recorded between 500 and 700 nm with excitation at 490 nm. A 1 cm path-length Suprasil quartz fluorescence cuvette was used for these measurements.

For measuring the rate of DNA damage induced by LED and DAC, 0.2 μM of each of the dsDNA sequences (Table 2) were mixed separately with 0.3 μM EG dye using buffer (10 mM

Tris, 10 mM NaCl, 1 mM EDTA, pH 7.5) in different 96-well microplates. The microplates were incubated at 37 °C for 20 min in the dark and left to cool for 1 hr at room temperature, then LED and DAC were added separately to dsDNA-EG mixture in separate wells within a concentration range of 0.01 – 100 μ M. Room-temperature fluorescence intensities were recorded every minute for a period of 24 hr using the Safire fluorescence plate reader with an excitation wavelength of 490 nm and an emission wavelength of 530 nm.

3. Results and Discussion

3.1. Absorption spectral studies.

Absorption spectroscopy is an effective method to examine the effect of different drugs and metal complexes on DNA. Any changes in the spectral features of DNA, such as hypo-/hyperchromism or batho-/hypsochromic shifts, reflect changes in the stacking interaction between different base pairs in the DNA, likely reflecting structural changes in the DNA that may be indicative of damage [23]. The absorption spectra of DNA in the presence of the five antiviral drugs studied here are presented in Figure 1. Results in Figure 1 show hyperchromicity in the characteristic 260 nm absorption band of DNA in the presence of ledipasvir (LED) and daclatasvir (DAC) that increase with incubation time (Figure 1a, b). No spectral changes are observed in the absence of these drugs (see supplementary information, Figure S1). The spectral changes of the DNA observed in the presence of DAC and LED reflects the occurrence of some sort of DNA-drug interaction that affects the base-pair stacking and therefore increases the DNA absorbance at 260 nm. For ribavirin (RIB), sofosbuvir (SOF) and tenofovir (TEN), no change in the 260 nm absorption band is observed (Figure 1c, d, and e) and therefore, these drugs are not considered

further in this study. This result is not surprising, due to the high structural resemblance of TEN, RIB, and SOF to the DNA nucleobases or nucleotides (Table 1).

Figure 1a additionally shows a decrease in the 330 nm absorption band of LED in the presence of DNA with increasing incubation time. This result is not observed for LED in the absence of DNA (supplementary information, Figure S1). No such spectral differences in the 315 nm absorption band of DAC in the presence (Fig. 1b) or absence (supplementary information, Figure S1) of DNA is observed with increasing incubation time. This result indicates that LED and DAC may exhibit two different mechanisms of interaction with DNA which nevertheless are common in affecting the stacking interaction between the base-pairs, causing an increase in the 260 nm absorption band. The absorption bands for RIB, SOF and TEN lie within the DNA absorption band, and no significant changes are observed for that band for these 3 drugs, as discussed above.

3.2. MALDI-TOF MS analysis of DNA in the presence of LED and DAC

In order to investigate the damage induced in DNA upon incubation with LED and DAC, MALDI-TOF MS was performed on the random DNA sequence (Table 2) incubated with LED and DAC at different time intervals. Figures 2 and 3 show the mass spectra of random DNA in the presence of LED and DAC, respectively. Figure 2a records the DNA mass spectrum immediately after mixing with LED. The signals at $m/z \sim 6,485$ are the molecular ions of each of the two complementary strands of the random DNA sequence. Smaller side peaks in Figure 2a represent the molecular ions non-covalently complexed with one or more sodium ($m/z=23$) and/or potassium ($m/z=39$) ions. Figure 2a shows no other significant peaks than the molecular ions of the DNA. Thus, no evidence of an immediate reaction between DNA and LED is seen in the mass spectrum. However, after 6 hr incubation with LED, Figure 2b shows a significant decrease in the molecular

ion peak of DNA at $m/z \sim 6,485$ with the subsequent appearance of four other, much higher-intensity peaks at smaller $m/z \sim 1,575, 1,739, 2,614,$ and $3,503$. After 24 hr incubation of DNA with LED (Figure 2c), the molecular ion peak of DNA completely disappears and the intensities of the other four lower m/z peaks have significantly increased. The insets in Figure 2 focus on the spectra in the region 1250–4000 to show the peaks produced upon the reaction of DNA with LED. DAC shows similar spectra and a similar progression of the mass spectrum with increasing DNA incubation time (Figure 3). The mass spectrum of the random DNA after immediate mixing with DAC shows only one molecular ion peak at $m/z \sim 6,445$ that corresponds to the two complementary strands of the random DNA sequence (Figure 3a). After 6 hr incubation, however, Figure 3b shows a significant decrease in the molecular ion peaks of DNA at $m/z \sim 6,445$ with the appearance of two other peaks at smaller $m/z \sim 1,478$ and $1,517$. The intensities of these two peaks increase significantly after the 24 hr incubation of DNA with DAC and the DNA molecular ion peaks are again almost completely absent (Figure 3c). The insets in Figure 3 focus on the spectral region 1200 – 2000 to show the resulting peaks produced upon the reaction of DNA with DAC.

It is clear from the spectra in Figure 2 and 3 that there are no peaks at an m/z greater than that of the molecular ion peak of the DNA. This indicates that the change in absorption spectra of DNA in the presence of LED and DAC (Figure 1) is not due to covalent modification or intercalation binding of the drugs with DNA. Instead, the mass spectra after long incubation time with the LED and DAC (Figure 2 and 3) show significant decreases in the molecular ion peak of DNA with the appearance of other peaks at smaller m/z that increase significantly with incubation time, hence the formation of smaller DNA fragments, likely caused by damage such as strand breaks. Moreover, the interaction of LED and DAC with DNA results in the formation of peaks with different m/z values indicating that the site of interaction of LED with DNA differs from that of DAC, which agrees with the different absorption results obtained (Figure 1a and b).

We propose that LED and DAC induce DNA strand breaks as a result of the oxidation of the deoxyribose moieties in the DNA. It has been previously reported that oxidative damage to the deoxyribose moieties is mainly through the formation of alkaline labile lesions resulting from oxidation at the DNA C-1' or C-4' positions [24] or through direct strand scission that occurs via an oxygen-dependent process initiated by C-4' hydrogen atom abstraction in DNA [25]. The resulting DNA fragments would thus have lower m/z values than the parent DNA.

3.3. Fluorescence spectroscopy: Determination of DNA damage induced by LED and DAC

Since LED and DAC are non-emissive both in the absence and presence of DNA, the fluorescent dye EvaGreen (EG) [22] was used for the determination of any DNA structural changes in the presence of LED and DAC. EG is constructed of two monomeric units joined through a flexible linker. This dimeric dye is fluorescently inactive in the absence of dsDNA and assumes a closed loop conformation with the two chromophores in close proximity to one another, which quenches any fluorescence. However, the closed loop conformation of EG opens upon binding to DNA, separating the two chromophores and leading to maximum fluorescence. Most importantly, the equilibrium between bound and free EG in the presence of DNA is substantially affected by DNA base pairing; disruptions to the normal base pairing leads to a reduction in EG fluorescence due to a shift of the equilibrium more to the free, non-fluorescent EG [22]. Figure 4a shows the fluorescence spectra of EG in the presence and absence of dsDNA after excitation at 490 nm. As expected, the dsDNA-EG complex shows high fluorescence intensity at 530 nm (Figure 4a, solid line) while no EG fluorescence is seen in the absence of dsDNA (Figure 4a, dotted line). Also, dsDNA does not show any fluorescence at 350 nm in the absence of EG (Figure 4a, dashed line).

Upon the addition of LED to the EG/dsDNA mixture and immediate fluorescence measurement, a high intensity fluorescence is recorded (Figure 4b, solid line). However, after 6 hr of incubation (Figure 4b, dashed line), a decrease in EG fluorescence was observed which further decreased after 24 hr of incubation (Figure 4b, dotted line). The same trend was observed for DAC with the dsDNA-EG mixture (Figure 4c), although the magnitude of decrease after 6 and 24 hrs is different for the two drugs. We interpret this decrease in fluorescence intensity to the decomplexation of EG from the dsDNA, likely due to DNA damage induced by the drugs. This conclusion is supported by the fact that no such change in fluorescence was observed with only dsDNA and EG (Figure 4b and 4c insets).

As shown in Figure 4, there is a good dynamic range in the fluorescence intensity with increasing drug-dsDNA incubation time for both LED and DAC. To further explore whether this decrease in fluorescent intensity can be correlated to the amount of damage produced, the kinetics of the drug-dsDNA interaction, detected by the changing EG fluorescence are shown in Figure 5 for LED (Figure 5a) and for DAC (Figure 5b). For comparison, the rate of decrease in fluorescence of the dsDNA-EG complex alone, the LED-/DAC-EG complex alone, LED/DAC alone, DNA alone and EG alone are also shown in Figure 5. The fluorescence intensity was recorded every minute over 24 hr in order to precisely characterize the EG fluorescence changes, and the structural changes in the DNA they reflect.

Figure 5a shows that EG has higher fluorescence intensity for the LED-dsDNA-EG mixture than that of the dsDNA-EG complex alone. This result may indicate that the presence of LED enhances intercalation of the EG dye into dsDNA, and thereby increases its emission through a concentration effect. It is unlikely that a direct interaction between LED and EG which enhances EG emission is occurring, since the EG-LED fluorescence trace is essentially at baseline and

unchanged throughout the entire 24 hr period (Figure 5a). For the first 150 min of incubation, the fluorescence intensity of the LED-dsDNA-EG mixture remains constant during which the drug-induced DNA damage is not sufficient to affect the intercalation of EG with DNA resulting in the initial constant fluorescence. After the first 150 min of incubation with LED, the fluorescence intensity decreases gradually and exponentially with increasing incubation time until the fluorescence reaches its minimum intensity after ~900 min incubation. This gradual decrease in fluorescence with time is interpreted as LED-induced DNA damage, which leads to decomplexation of EG with a consequent decrease in fluorescence emission. This interpretation is consistent with both the absorption and mass spectral data presented above. After 900 min incubation, the fluorescence intensity of the LED-dsDNA-EG mixture remains constant and overlaps the LED-EG fluorescence plot until the end of the 24 hr measurements, which indicates that all the EG is completely released after 15 hr (900 min) of DNA incubation with LED. On the other hand, the fluorescence intensity of the dsDNA-EG sample remains essentially constant throughout the measurement, as did the kinetic traces of LED/DAC alone, DNA alone and EG alone; these latter samples showed minimal fluorescence that did not change with incubation time.

Similarly, Figure 5b shows that the fluorescence intensity of the DAC-dsDNA-EG mixture remains constant for the first 400 min incubation. This indicates that DAC requires a longer "latency" time than LED before EG begins decomplexation from the dsDNA. After ~400 min incubation, the EG fluorescence intensity gradually decreases with incubation time until the fluorescence reaches its minimum intensity at ~900 min of incubation. At this time, the dsDNA-EG-DAC fluorescence is the same as the DAC-EG fluorescence and continues at this minimal fluorescence intensity level until the end of the measurements. Thus, EG has completely decomplexed from the dsDNA on the same timescale for DAC as for LED, but with different

damage kinetics. The different latency time and different rate constant for the subsequent damage between the two drugs again emphasizes that the actual damage mechanism is different for the two, but that both damage the dsDNA.

To further characterize the interaction of dsDNA with the two antiviral drugs, LED and DAC, fluorescence kinetics as a function of drug concentration were measured. Figure S2 in the supplementary information shows the results of these studies over the 0-100 μM concentration range for LED (Fig. S2a) and DAC (Fig. S2b). All plots in Figure S2 show an increase in the initial fluorescence of the dsDNA-EG complex as the concentration of the drug increases, consistent with a drug-induced, concentration-dependent shift of the complexation equilibrium towards the dsDNA-EG complex. Similar to Figure 5, EG decomplexation from the dsDNA proceeds after a latency period, with the latency period shorter and the decomplexation kinetics faster as the drug concentration increases. The kinetics of the dsDNA-EG fluorescence decrease after the initial latency periods for each drug concentration was fit to a single exponential function in order to determine the rate of decrease of fluorescence intensity with incubation time. The single exponential function used is

$$I_F = I_{F0} + Ae^{-t/\tau}$$

where I_F is the fluorescence intensity at time t , I_{F0} is the fluorescence intensity at time 0, A is the amplitude, and $e^{-t/\tau}$ is the exponential decay with τ representing the damage constant. Table S1 in the supplementary information shows all the fitting parameters obtained. The insets in Figure S2 show a representative example of the exponential fit to the data points of the rate of DNA damage induced by 10 μM LED (Figure S2a-inset) and 10 μM DAC (Figure S2b-inset). All the exponential fits to the rate of DNA damage induced by different concentrations of LED and DAC are presented

in Figure S3 and S4 in the supplementary material. The faster the decrease in the fluorescence intensity with time, the smaller the damage constants (τ) obtained from the exponential fits and the faster the rate of DNA damage induced by the drug. Figure 6 and Table S1 show that as the concentration of LED or DAC increases, the damage constant generally decreases, reflecting the greater rate of damage induced in DNA. Thus, different drug concentrations could be chosen according to the required degree of efficacy as an anticancer drug

In order to get some insight into the dsDNA damage mechanism for LED and DAC, the rate of EG fluorescence change, reflecting structural changes likely due to damage, was studied by incubating four different sequences of dsDNA with LED and DAC for 24 hr. The four dsDNA sequences (Table 2) include a random sequence with 18 guanines (G's)/ cytosines (C's) base pairs and 3 thymines (T's)/adenines (A's) base pairs, a poly-TG sequence with 10 G/C base pairs and 11 T/A base pairs, a poly-TC sequence with 10 G/C base pairs and 11 T/A base pairs and finally, a poly-T sequence with 21 T/A base pairs. Figure S5 in the supplementary information shows the rate of fluorescence decrease upon incubation of DNA with each of the two drugs. All dsDNA sequences have been subjected to the same conditions during the experiment and incubated with 100 μ M of each drug. Initially at the latency period, the poly-TG sequence with both LED and DAC has the highest initial fluorescence intensity of all the four sequences, followed by the poly-TC sequence, then the random sequence and finally the poly-T sequence exhibits the lowest enhancement of EG fluorescence. This result indicates that EG dye intercalates best in DNA regions of alternating T and G bases and alternating T and C bases.

A comparison of the rates of fluorescence decrease provides a direct comparison of the influence of the different dsDNA sequence on the extent of damage induced by the antiviral drugs. The fluorescence plots of both LED (Figure S5a) and DAC (Figure S5b) are fit using the single

exponential function mentioned above. The exponential fits are presented in Figure S6 and S7 in the supplementary information and the damage constants of different sequences are listed in Table S2 in the supplementary information. The drug-induced damage rates seem to be similar for both LED and DAC as a function of sequence, with much smaller differences in the damage constant as a function of sequence than as a function of concentration. The damage constants listed in show that the random sequence has a somewhat smaller damage constant than the poly-TG and poly-TC sequences, which have very similar damage constants, while the poly-T sequence has a somewhat higher damage constant than all the other sequences. This result suggests that the random sequence is damaged faster by the antiviral drugs than the other three sequences and the poly-T sequence is damaged slower than the other three sequences. Comparing nucleobases in each sequence reveals that the random sequence has 18 G's which are most prone to oxidative damage, suggested here to be the mechanism of DNA damage induced by LED and DAC. However, poly-TG and poly-TC sequences have only 10 G's and the poly-T sequence has no G's at all, which is consistent with the ranked order of increase in the damage constants (Table S2) in this oxidative damage model. Guanine has the lowest ionization potential among all DNA components; it serves as the preferred site of electron loss in DNA with subsequent formation of the guanine cation radical [26]. This radical undergoes nucleophilic addition of water at C8 to form the 8-hydroxy-7,8-dihydroguanine-7-yl radical that either loses one electron to form 8-oxo-guanine or gains one electron to form the formamidopyrimidine product [27]. The formation of these DNA lesions may likely affect the Watson-Crick base pairing of the dsDNA sequences, and lead to decomplexation of EG from the damaged DNA, forming the minimally emissive free EG. The greater the number of G's in the DNA, the faster the rate of damage and the lower the subsequent fluorescence emission at a specific incubation time.

This study demonstrates the DNA damaging effect of the two antiviral drugs, LED and DAC. These drugs present a promising therapeutic approach for HepB and HepC patients with hepatocellular carcinoma unable to be treated with other therapies. These two antiviral drugs have the potential to be used as targeted therapies with dual antiviral and anticancer activities, especially for cases resistant to conventional approaches. HepC-infected cells have been reported to be resistant to DNA-damage-induced apoptosis where several HepC components can inhibit the activation of p53 gene in the nucleus [28-30] and therefore most of the HepC patients are highly prone to hepatocellular carcinoma. Our results show that LED and DAC induce DNA damage, likely through the oxidation of both nucleobases and deoxyribose moieties of DNA. However, the exact mechanism of damage requires more study and further investigation using a variety of tools such as ^{18}O -labeling, ^3H -labeling and product analysis. Also, more research needs to be done to evaluate the drug-induced DNA damage in cells using techniques such as PCR, fluorescence in situ hybridization, flow cytometry, gel electrophoresis and comet assays, and to study the efficacy and dose response of these antiviral drugs as anticancer agents in experimental animals.

4. Conclusion

Five newly developed FDA-approved antiviral agents, ribavirin, sofosbuvir, tenofovir disoproxil fumarate, daclatasvir and ledipasvir, were studied in this work to probe their DNA-damaging potential and mechanism. The drug-induced DNA damage has been examined using absorption spectroscopy, MALDI-TOF mass spectroscopy, and fluorimetric analysis using EG, an intercalating dye. The major conclusion of the present study is that ledipasvir and daclatasvir can induce nucleic acid damage. The absorption spectra show hyperchromicity in the 260 nm absorption band characteristic to DNA that increases with incubation time with ledipasvir and daclatasvir. The mass spectrometric results show a disappearance of the DNA molecular ion peak

with the appearance of other peaks with smaller m/z , likely due to DNA strand breaks upon incubation with ledipasvir or daclatasvir. Furthermore, fluorimetric analysis using the EG dye has been used to measure the rate of the drug-induced DNA damage upon incubation with the two studied drugs. The results show that the rate of DNA-induced damage is dependent on the concentration of the antiviral drug and that DNA regions rich in guanine appear to be slightly more susceptible to ledipasvir- and daclatasvir-induced damage, which suggests that ledipasvir and daclatasvir may induce oxidative damage to DNA. This work is considered to be the first study to suggest a novel approach for the treatment of hepatitis B and C patients with hepatocellular carcinoma, especially for those cases that are resistant to conventional treatment approaches.

5. Acknowledgements

The authors acknowledge financial support for this work from the Canadian Natural Sciences and Engineering Research Council (NSERC) Discovery Grants-in-aid programme and the University of Alberta Faculty of Science.

6. References:

1. S. Mittal, H.B. El-Serag, Epidemiology of hepatocellular carcinoma: consider the population. *J. Clin. Gastroenterol.* 47 (2013) S2 - S6.
2. H.B. El-Serag, Epidemiology of viral hepatitis and hepatocellular carcinoma, *Gastroenterol.* 142 (2012) 1264 -1273.
3. S.P. Hiotis, N.N. Rahbari, G.A. Villanueva, E. Klegar, W. Luan, Q. Wang, H.T. Yee, Hepatitis B vs. hepatitis C infection on viral hepatitis-associated hepatocellular carcinoma, *BMC Gastroenterol.* 64 (2012) 1-7.
4. J.F.Perz, G.L.Armstrong, L.A.Farrington, Y.J.F. Hutin, B.P.Bell, The contributions of hepatitis B virus and hepatitis C virus infections to cirrhosis and primary liver cancer worldwide, *J. Hepatol.* 45 (2006) 529-538.
5. S. Fujimaki, Y. Matsuda, T. Wakai, A. Sanpei, M. Kubota, M. Takamura, S. Yamagiwa, M. Yano, S. Ohkoshi, Y. Aoyagi, Blockade of ataxia telangiectasia mutated sensitizes

- hepatoma cell lines to sorafenib by interfering with Akt signaling, *Cancer Lett.* 319 (2012) 98-108.
6. C. Kamphues, N. Al-Abadi, A. Durr, R. Bova, F. Klauschen, A. Stenzinger, M. Bahra, H. Al-Abadi, P. Neuhaus, D. Seehofer, The DNA index is a strong predictive marker in intrahepatic cholangiocarcinoma: the results of a five-year prospective study, *Surg. Today* 44 (2014) 1336-1342.
 7. F. Arjmand, S. Parveen, M. Afzal, L. Toupet, T.B. Hadda, Molecular drug design, synthesis and crystal structure determination of Cu^{II}-Sn^{IV} heterobimetallic core: DNA binding and cleavage studies, *Eur. J. Med. Chem.* 49 (2012) 141-150
 8. M. Chauhan, K. Banerjee, F. Arjmand, DNA binding studies of novel copper(II) complexes containing L-tryptophan as chiral auxiliary: In vitro antitumor activity of Cu-Sn₂ complex in human neuroblastoma cells, *Inorg. Chem.* 46 (2007) 3072-3082
 9. B. Rosenberg, L. VanCamp, J.E. Trosko, V.H. Mansour, Platinum compounds: a New class of potent antitumour agents, *Nature* 222 (1969) 385-386.
 10. S. Sauvaigo, T. Douki, F. Odin, S. Caillat, J-L. Ravanat, J. Cadet, Analysis of Fluoroquinolone-mediated Photosensitization of 2'-Deoxyguanosine, Calf Thymus and Cellular DNA: Determination of Type-I, Type-II and Triplet-Triplet Energy Transfer Mechanism Contribution, *Photochem. Photobiol.* 73 (2001) 230-237
 11. N. Shahabadi, L. Heidari, Binding studies of the antidiabetic drug, metformin to calf thymus DNA using multispectroscopic methods, *Spectrochim. Acta A Mol. Biomol. Spectrosc.* 97 (2012) 406-410
 12. J.A. War, S.K. Srivastava, S.D. Srivastava, Design, synthesis and DNA-binding study of some novel morpholine linked thiazolidinone derivatives., *Spectrochim. Acta A Mol. Biomol. Spectrosc.* 173 (2017) 270-278
 13. U. Pindur, M. Jansen, T. Lemster, Advances in DNA-ligands with groove binding, intercalating and/or alkylating activity: chemistry, DNA-binding and biology, *Curr. Med. Chem.* 12 (2005) 2805-2847.
 14. R. Focaccia, R.F.de Mello, P.S. Montes, F.M. Conti, Management of Hepatitis C Infection with Direct Action Antiviral Drugs (DAA), *Arch. Hepat. Res.* 1 (2016) 9-17.
 15. T. Biver, F. Secco, M.R. Tine, M. Venturini, Kinetics and equilibria for the formation of a new DNA metal-intercalator: the cyclic polyamine Neotrien/copper(II) complex, *J. Inorg. Biochem.* 98 (2004) 33-40.
 16. C. Liu, J. Zhou, H. Xu, Interaction of the copper(II) macrocyclic complexes with DNA studied by fluorescence quenching of ethidium, *J. Inorg. Biochem.* 71 (1998) 1-6.
 17. A.F. El-Yazbi, A. Wong, G.R. Loppnow, A luminescent probe of mismatched DNA hybridization: Location and number of mismatches, *Analytica Chimica Acta* 994 (2017) 92-99
 18. Z.J. Shire, G.R. Loppnow, Molecular beacon probes for the detection of cisplatin-induced DNA damage, *Anal. Bioanal. Chem.* 403 (2012) 179-184

19. S. Mahadevan, M. Palaniandavar, Spectroscopic and voltammetric studies of copper(II) complexes of bis(pyrid-2-yl)-di/trithia ligands bound to calf thymus DNA, *Inorg. Chim. Acta* 254 (1997) 291-302.
20. C.A. Mitsopoulou, C.E. Dagas, C. Makedonas, Synthesis, Characterization, DNA Binding, and Photocleavage Activity of Oxorhenium (V) Complexes with α -Diimine and Quinoxaline Ligands, *Inorg. Chim. Acta* 361 (2008) 1973-1982.
21. W. Wang, K. Chen, C. Xu, DNA quantification using EvaGreen and a real-time PCR instrument, *Anal. Biochem.* 356 (2006) 303-305.
22. L. C. T. Shoute and G. R. Loppnow Characterization of the binding interactions between EvaGreen dye and dsDNA, *Phys. Chem. Chem. Phys. Issue 7, 2018* DOI: 10.1039/c7cp06058k
23. V.A. Bloomfield, D.M. Crothers, I. Tinoco, *Physical Chemistry of Nucleic Acids*, Harper and Row, New York, 1974.
24. P.J. McHugh, J. Knowland, Novel reagents for chemical cleavage at abasic sites and UV photoproducts in DNA, *Nucl. Acid Res.* 23 (1995) 1664-1670
25. M.M. Greenburg, Chemistry of DNA Damage, in: O. Meth-Cohn, S.D. Barton, K. Nakanishi (Eds.), *Comprehensive Natural Products Chemistry*, Volume 7, Elsevier Science Ltd., Amsterdam, 1999, pp. 372 – 425
26. C.J. Burrows, J.G. Muller, Oxidative Nucleobase Modifications Leading to Strand Scission, *Chem. Rev.* 98 (1998) 1109-1151.
27. P. Cheng, Y. Li, S. Li, M. Zhang, Z. Zhou, Collision-induced dissociation (CID) of guanine radical cation in the gas phase: an experimental and computational study, *Phys. Chem. Chem. Phys.* 12 (2010) 4667-4677.
28. I.S. Smirnova, N.D. Aksenov, E.V. Kashuba, P. Payakurel, V.V. Grabovetsky, A.D. Zaberezhny, M.S. Vonsky, L. Buchinska, P. Biberfeld, J. Hinkula, M.G. Isaguliant, Hepatitis C Virus Core Protein Transforms Murine Fibroblasts by Promoting Genomic Instability, *Cell Oncol.* 28 (2006) 177-190.
29. M. Majumder, A.K. Ghosh, R. Steele, R. Ray, R.B. Ray, Hepatitis C Virus NS5A Physically Associates with p53 and Regulates p21/waf1 Gene Expression in a p53-Dependent Manner, *J. Virol.* 75 (2001) 1401-1407.
30. T. Nishimura, M. Kohara, K. Izumi, Y. Kasama, Y. Hirata, Y. Huang, M. Shuda, C. Mukaidani, T. Takano, Y. Tokunaga, H. Nuriya, M. Satoh, M. Saito, C. Kai, K. Tsukiyama-Kohara, Hepatitis C Virus Impairs p53 via Persistent Overexpression of 3 β -Hydroxysterol Δ 24-Reductase, *J. Biol. Chem.* 284 (2009) 36442-36452.

Table 1. Structure and systematic names of the five antiviral drugs used in this study.

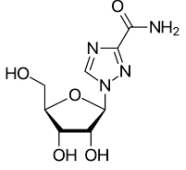
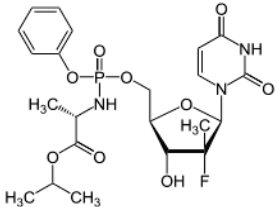
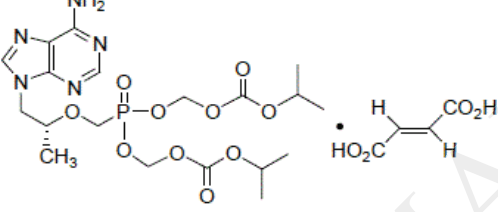
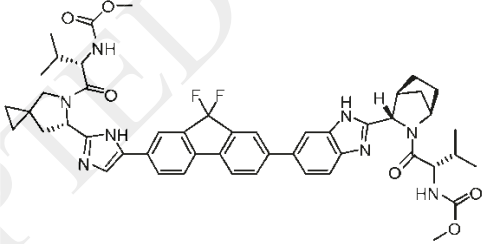
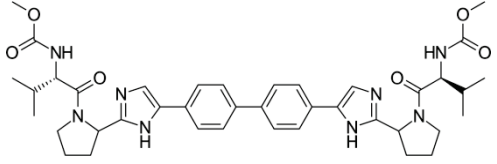
Name	Structure and IUPC name
Ribavirin (RIB)	 <p>1-[(2R,3R,4S,5R)-3,4-dihydroxy-5-(hydroxymethyl)oxolan-2-yl]-1H-1,2,4-triazole-3-carboxamide</p>
Sofosbuvir (SOF)	 <p>Isopropyl(2S)-2-[[[(2R,3R,4R,5R)-5-(2,4-dioxypyrimidin-1-yl)-4-fluoro-3-hydroxy-4-methyl-tetrahydrofuran-2-yl]methoxy-phenoxy-phosphoryl]amino]propanoate</p>
Tenofovir disoproxil fumarate (TEN)	 <p>Bis {[(isopropoxycarbonyl)oxy]methyl} { [(2R)-1-(6-amino-9H-purin-9-yl)-2-propanyl]oxymethyl}phosphonate (2E)-2-butenedioate</p>
Ledipasvir (LED)	 <p>MethylN-[(2S)-1-[(6S)-6-[5-[9,9-Difluoro-7-[2-[(1S,2S,4R)-3-[(2S)-2-(methoxycarbonylamino)-3-methylbutanoyl]-3-azabicyclo[2.2.1]heptan-2-yl]-3H-benzimidazol-5-yl] fluorene-2-yl]-1H-imidazol-2-yl]-5-azaspiro[2.4]heptan-5-yl]-3-methyl-1-oxobutan-2-yl]carbamate</p>
Daclatasvir (DAC)	 <p>Dimethyl N,N'-([1,1'-biphenyl]-4,4'-diylbis {1H-imidazole-5,2-diyl-[(2S) pyrrolidin - 2,1- diyl] [(2S)-3-methyl-1-oxobutane-1,2-diyl]})dicarbamate</p>

Table 2. Sequences of the dsDNA used in this study.

	Sequence
Random	5'-AGC CCG TCG GGC GGG AGC GCC-3' 3'-TCG GGC AGC CCG CCC TCG CGG-5'
poly-TG	5'-TGT GTG TGT GTG TGT GTG TGT-3' 3'-ACA CAC ACA CAC ACA CAC ACA-5'
poly-TC	5'-TCT CTC TCT CTC TCT CTC TCT-3' 3'-AGA GAG AGA GAG AGA GAG AGA-5'
poly-T	5'-TTT TTT TTT TTT TTT TTT TTT-3' 3'-AAA AAA AAA AAA AAA AAA AAA-5'

Figure legends:

Figure 1. The absorption spectra of the random oligonucleotide sequence (0.5 μM) in the presence of 20 μM of (a) LED, (b) DAC, (c) RIB, (d) SOF and (e) TEN in buffer (10 mM Tris, 10 mM NaCl, 1 mM EDTA, pH 7.5) for time intervals of 0 (solid line), 6 (dashed line) and 24 hr (dotted line).

Figure 2. MALDI-TOF MS of the random oligonucleotide in the presence of LED (a) immediately after mixing, (b) after 6 hr, and (c) after 24 hr incubation. The signal at $m/z \sim 6,485$ amu is the molecular ion of the random sequence.

Figure 3. MALDI-TOF MS of the random oligonucleotide in the presence of DAC (a) immediately after mixing, (b) after 6 hr, and (c) after 24 hr incubation. The signal at $m/z \sim 6,445$ amu is the molecular ion of the random sequence.

Figure 4. Fluorescence spectra of EG (a) in the presence (solid line) and absence (dotted line) of dsDNA, (b) after mixing with dsDNA and incubating with LED for 0 (solid line), 6 (dashed line) and 24 hr (dotted line), and (c) after mixing with dsDNA and incubating with DAC for 0 (solid line), 6 (dashed line) and 24 hr (dotted line). The final concentrations are 0.2 μM dsDNA, 0.3 μM EG and 10 μM LED or DAC in buffer (10 mM Tris, 10 mM NaCl, 1 mM EDTA, pH 7.5). Insets in Figure 4(b) and (c) represent the fluorescence spectra of the DNA-EG complex in the absence of the drugs measured at time intervals 0, 6 and 24 hr. The excitation wavelength is 490 nm and c.p.s. represents counts per second. The dashed line in Fig. 4a shows the fluorescence of dsDNA alone for comparison.

Figure 5. EG fluorescence intensity of the dsDNA-EG complex as a function of incubation time with (a) LED and (b) DAC (black line). EG fluorescence of the LED/DAC-EG complex (olive

green line), LED/DAC alone (cyan line), DNA alone (magenta dashed-dotted-dotted line) and EG alone (blue line) are also shown. The red line represents the dsDNA-EG complex without either of LED or DAC. The excitation wavelength is 490 nm and the emission wavelength is 530 nm. c.p.s. represents counts per second.

ACCEPTED MANUSCRIPT

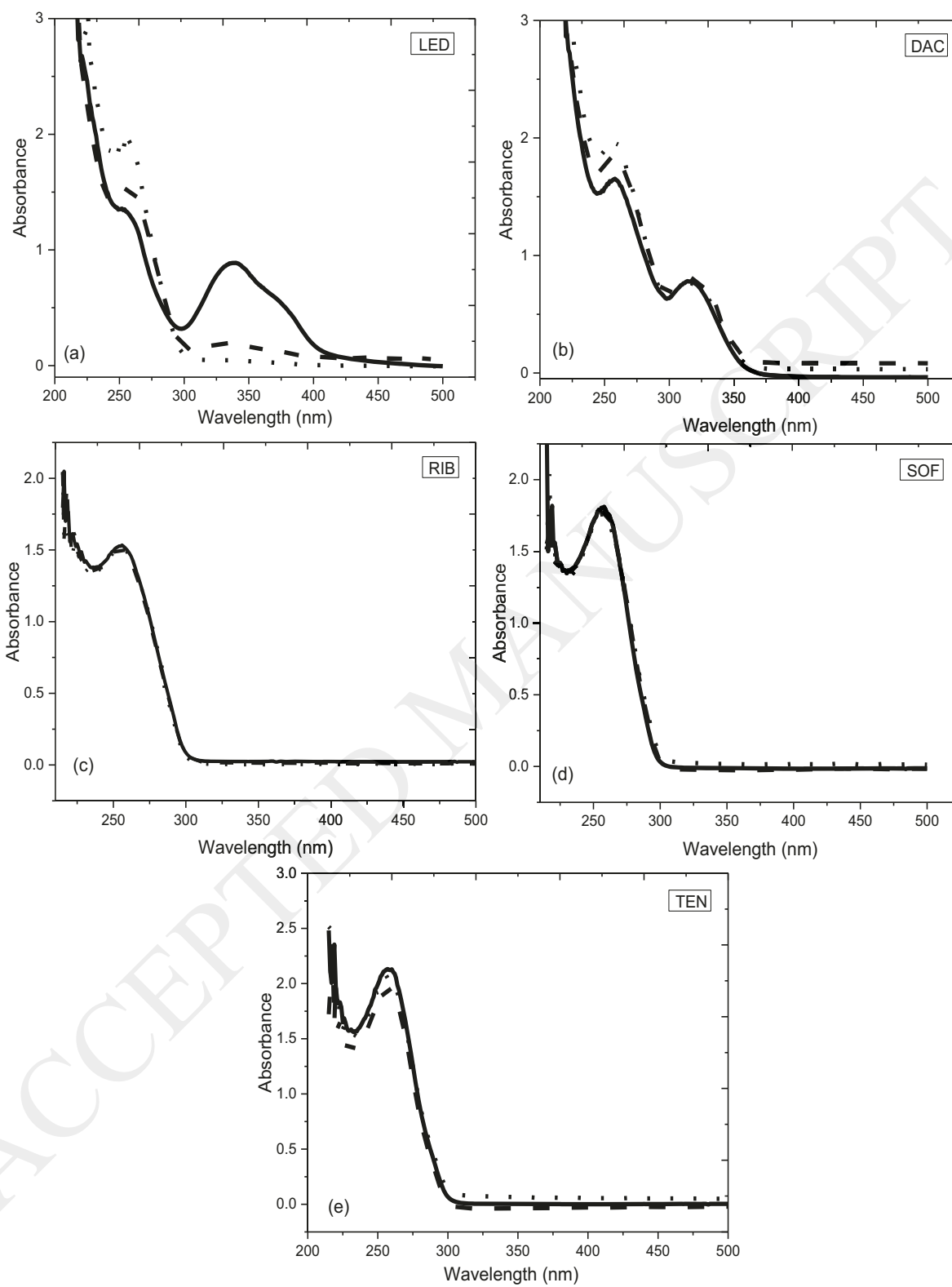


Figure 1

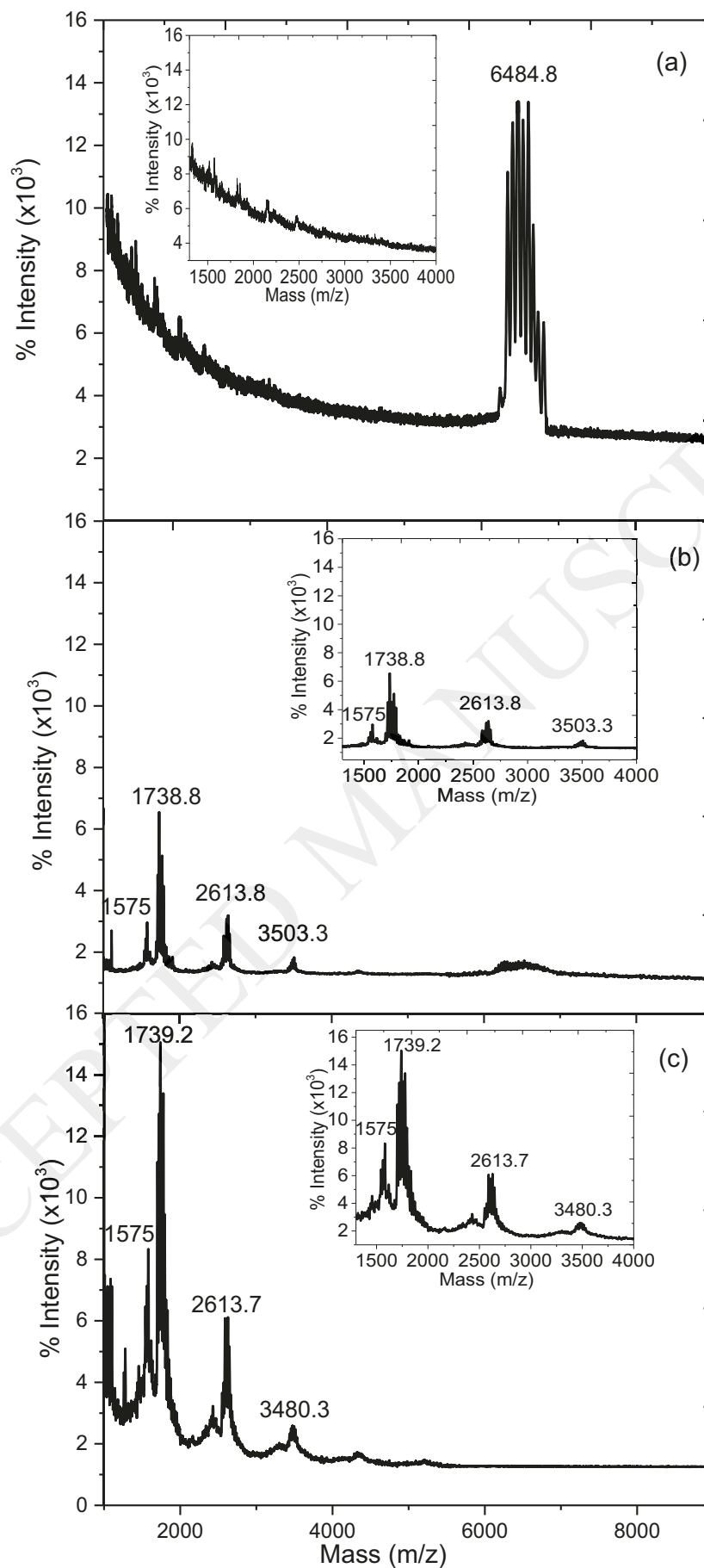


Figure 2

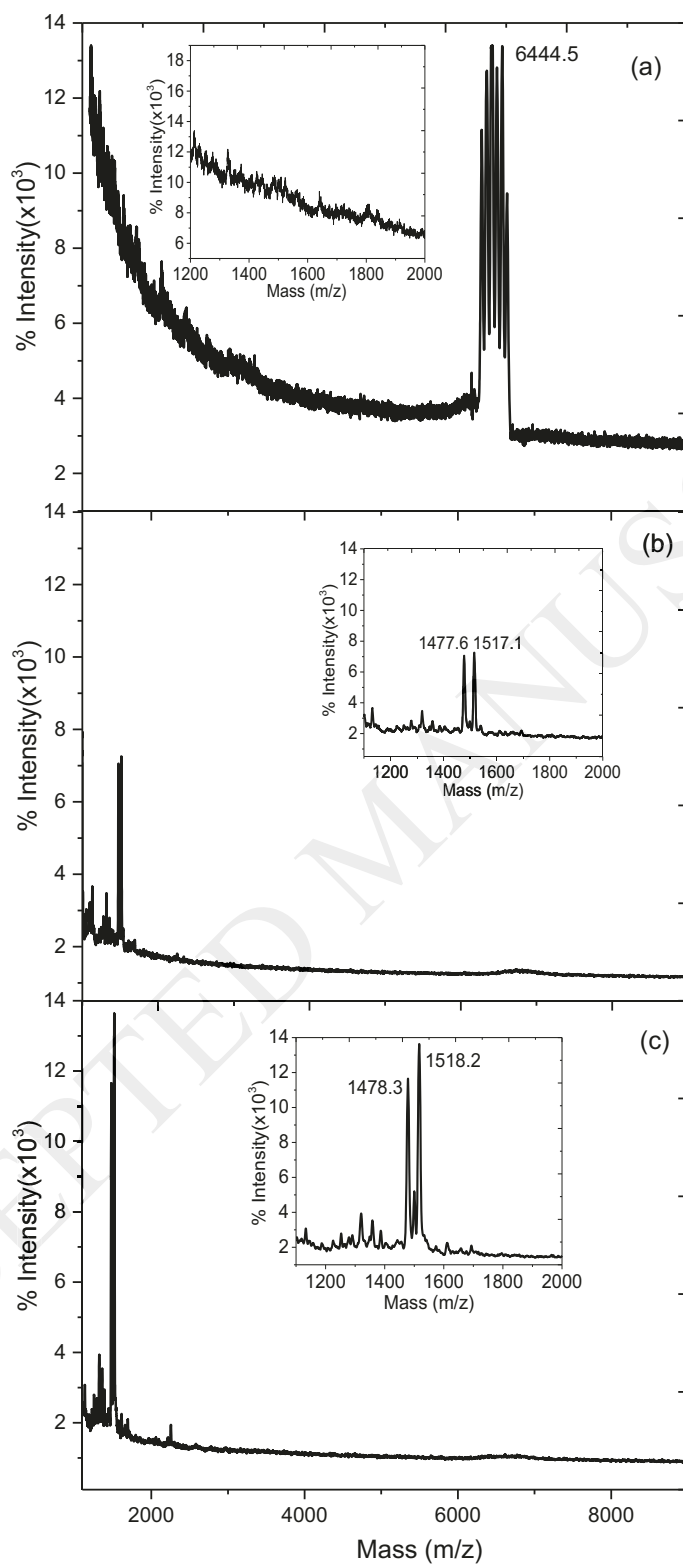


Figure 3

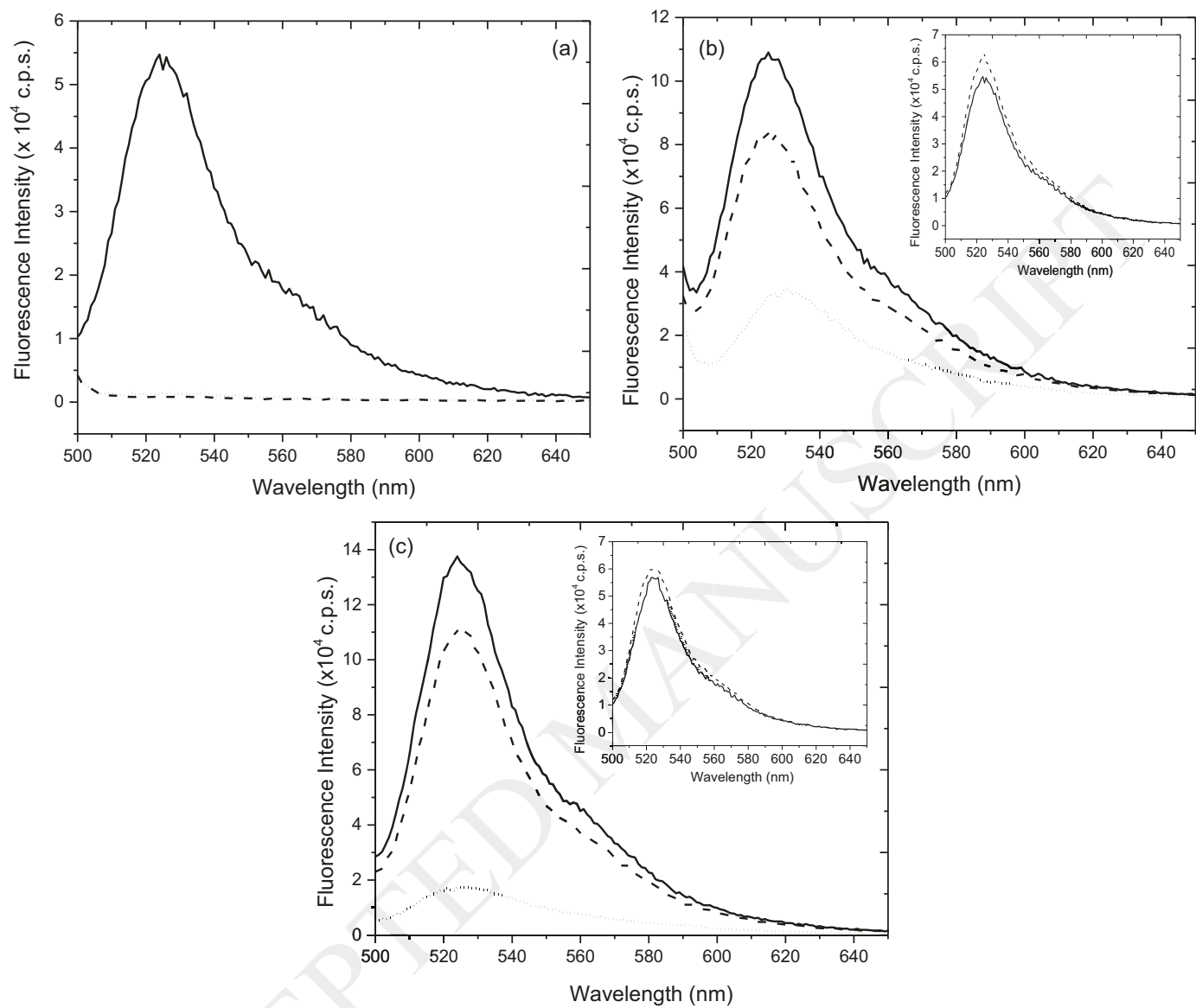


Figure 4

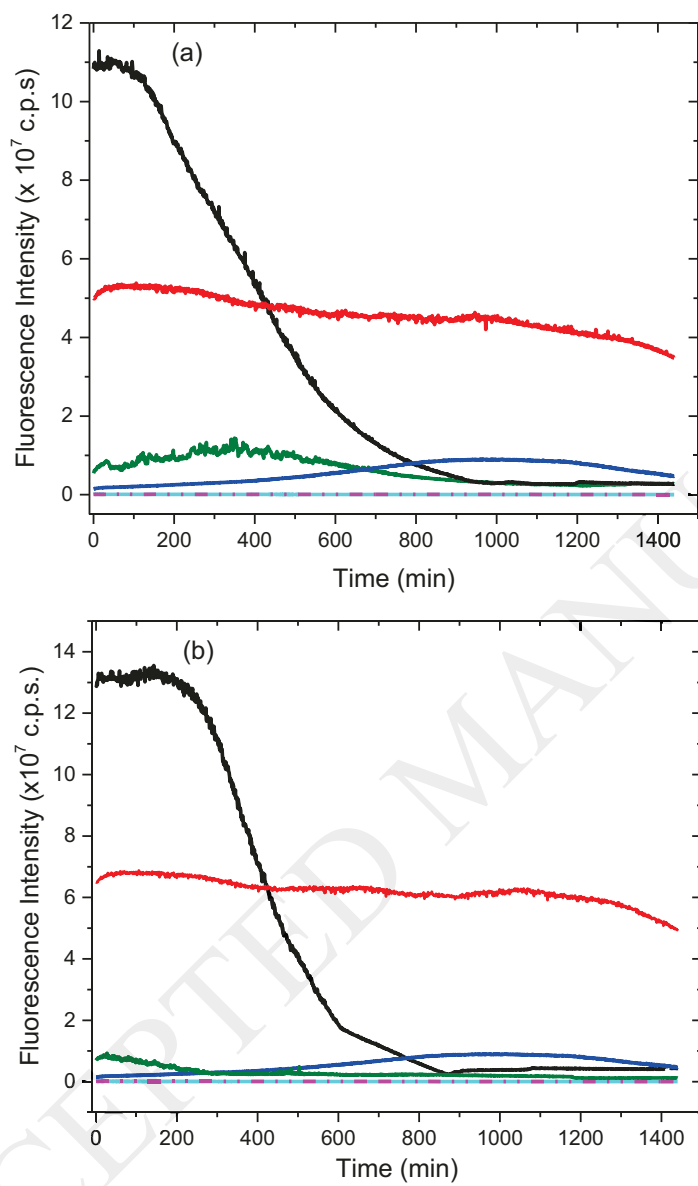


Figure 5

Supplementary Information

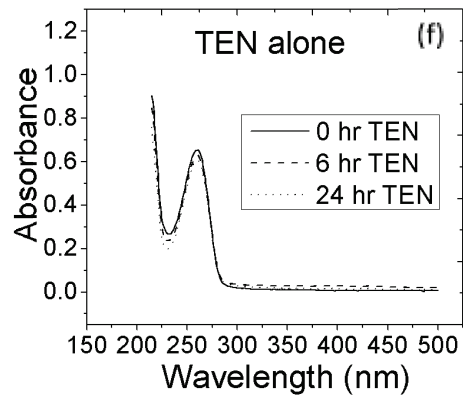
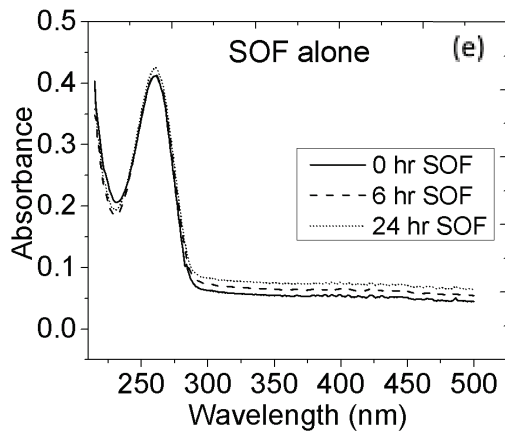
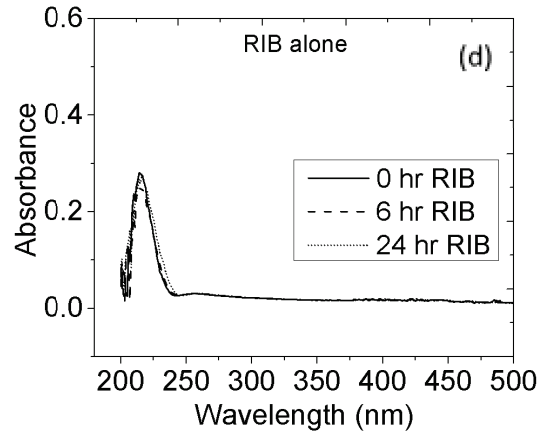
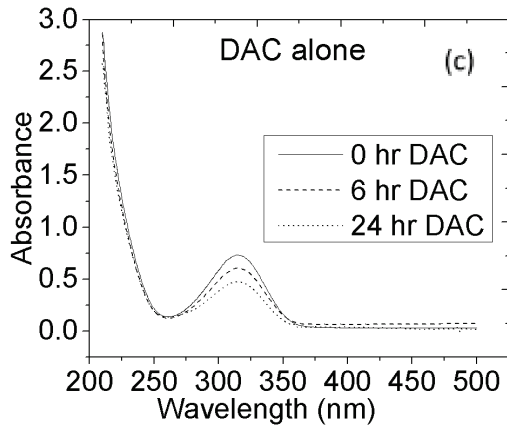
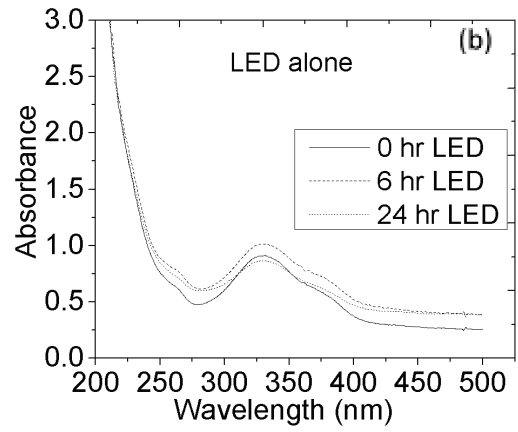
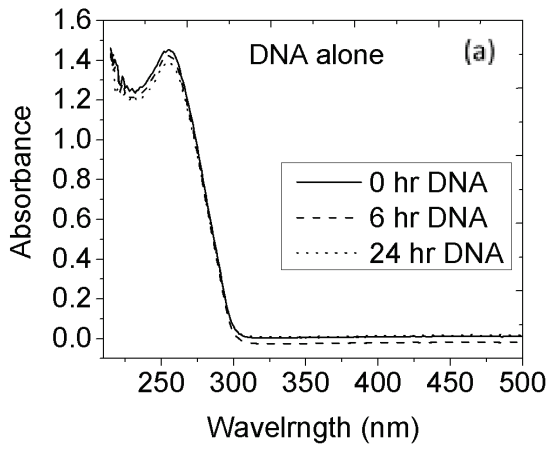


Figure S1: The absorption spectra of (a) the random oligonucleotide sequence (0.5 μM) alone, (b) LED, (c) DAC, (d) RIB, (e) SOF, (f) TEN in buffer (10 mM Tris, 10 mM NaCl, 1 mM EDTA, pH 7.5) for time intervals of 0 (solid line), 6 (dashed line) and 24 hr (dotted line).

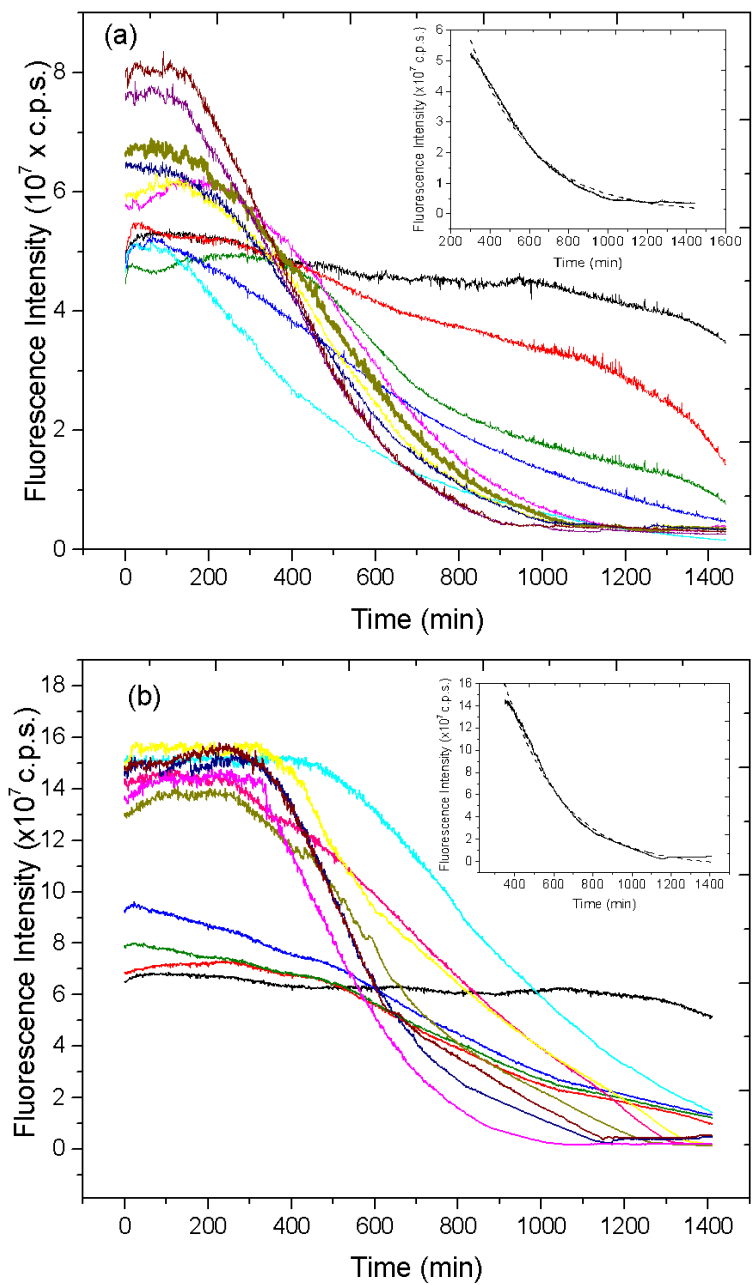


Figure S2. EG fluorescence intensity as a function of incubation time of 0.2 μM dsDNA mixed with 0.3 μM EG in the presence of different drug concentrations for (a) LED and (b) DAC. Different colored lines represent different drug concentrations with the dsDNA-EG complex such as 0 μM LED or DAC (black line), 0.01 μM LED or DAC (red line), 0.1 μM LED or DAC (olive line), 1 μM LED or DAC (blue line), 10 μM LED or DAC (cyan line), 20 μM LED or DAC (pink line), 30 μM LED or DAC (yellow line), 40 μM LED or DAC (dark yellow line), 60 μM LED or DAC (navy line), 80 μM LED or DAC (magenta line), 100 μM LED or DAC (wine line). The excitation wavelength is 490 nm and the emission wavelength is 530 nm. Insets in Figure 6a and 6b represent the single exponential fit to the equation $I_F = I_{F,0} + Ae^{-t/\tau}$ for dsDNA damage and 10 μM LED or 10 μM DAC, respectively. The damage constants (τ), offsets ($I_{F,0}$) and amplitudes (A) for each of the different concentrations are recorded in [Table S1 in the supporting information](#). c.p.s. represents counts per second.

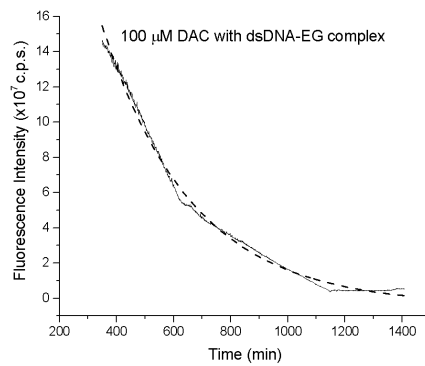
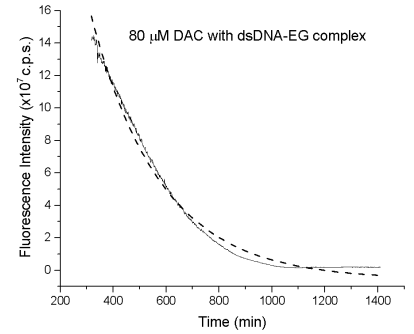
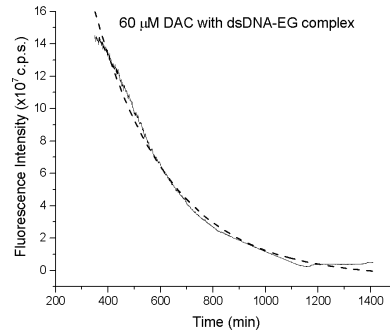
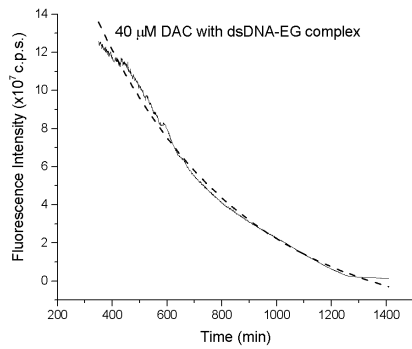
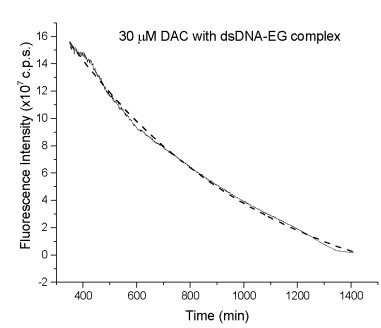
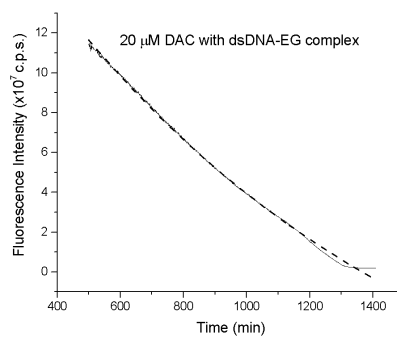
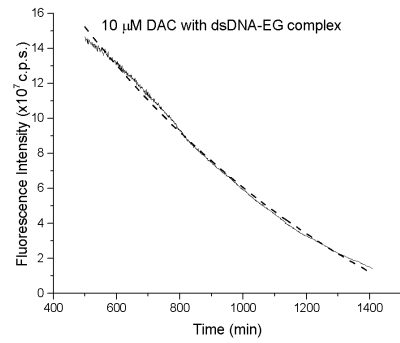
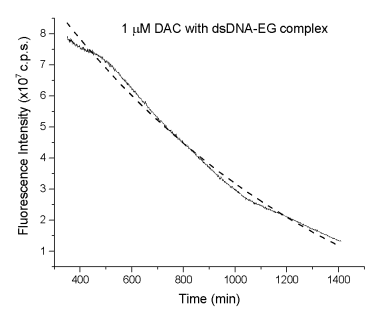
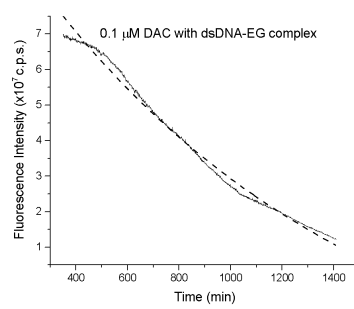
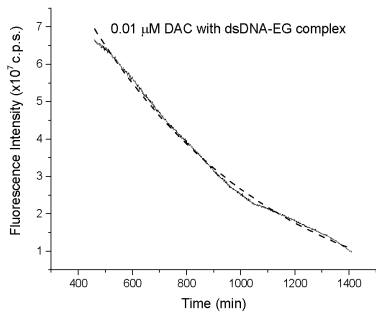
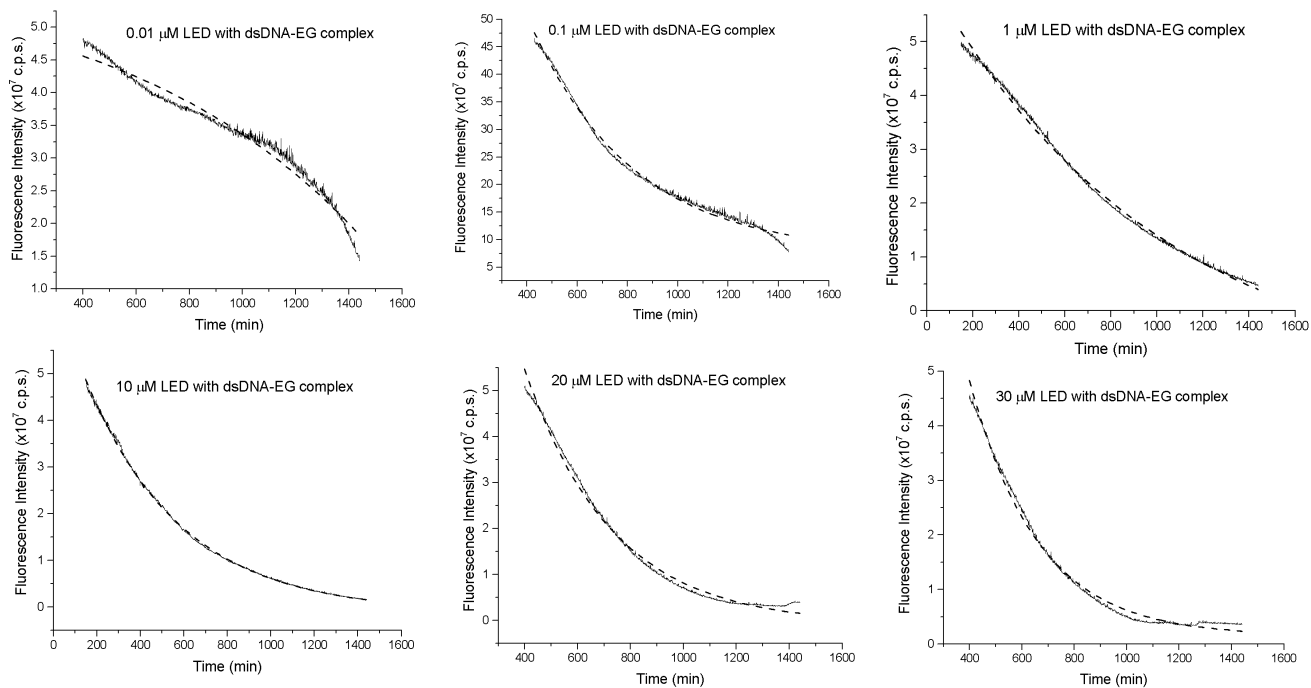


Figure S3: Effect of different concentration of DAC on the rate of DNA damage



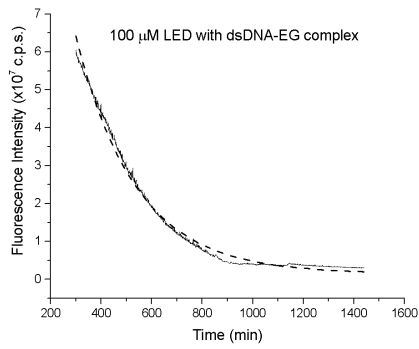
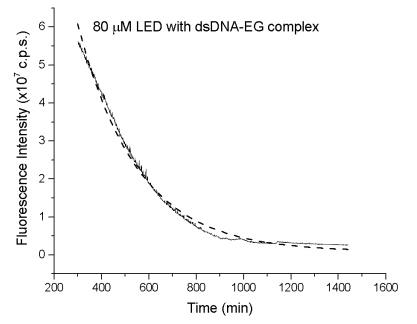
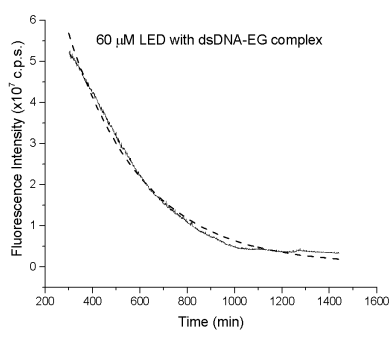
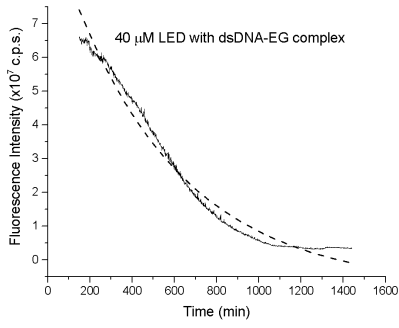
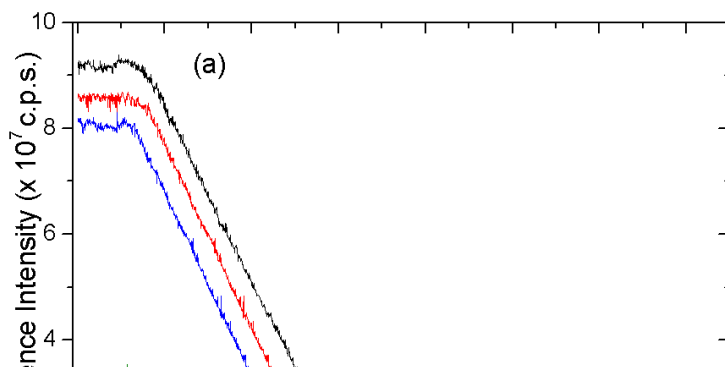


Figure S4: Effect of different concentration of LED on the rate of DNA damage



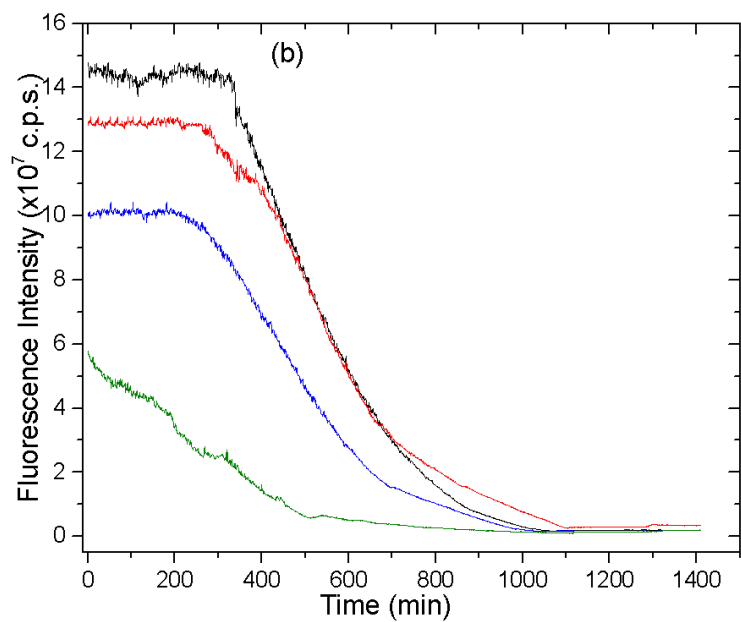
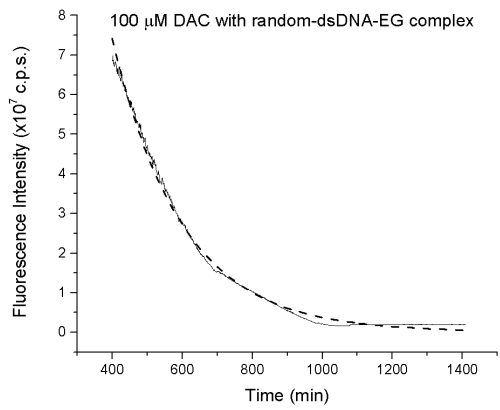
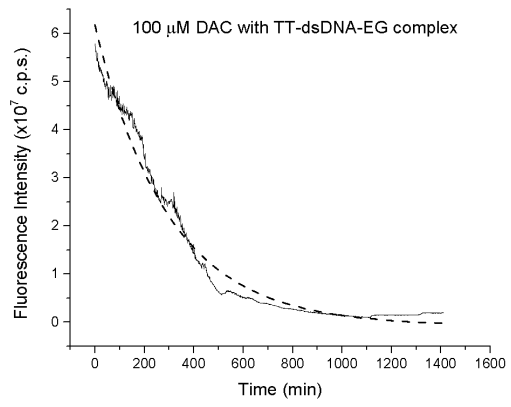


Figure S5. EG fluorescence intensity as a function of incubation time of 0.2 μM random (blue line), 0.2 μM poly-TG (black line), 0.2 μM poly-TC (red line) and 0.2 μM poly-T (olive line) sequences mixed with 0.3 μM EG in the presence of 100 μM of (a) LED and (b) DAC. All dsDNA sequences have been subjected to the same conditions during the experiment. The excitation wavelength is 490 nm and the emission wavelength is 530 nm. c.p.s. represents counts per second.



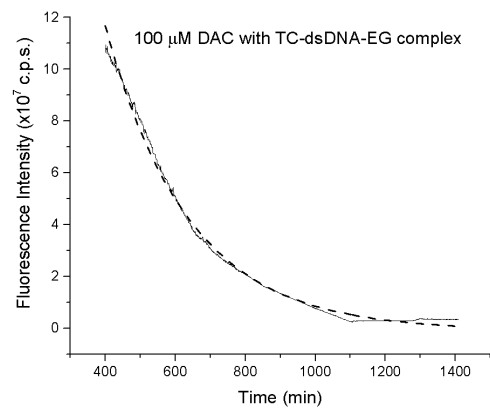
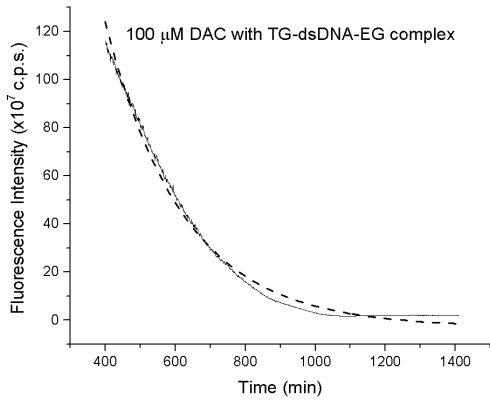


Figure S6: Effect of DAC on the rate of DNA damage of different dsDNA targets

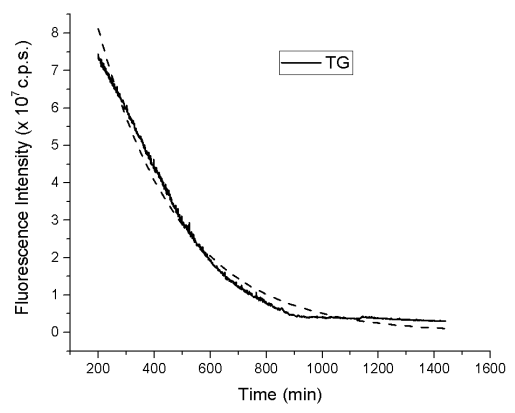
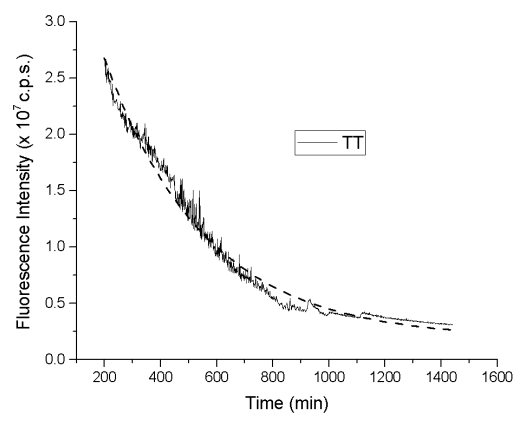
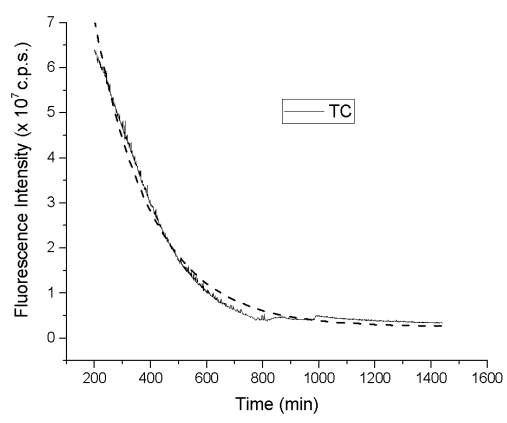
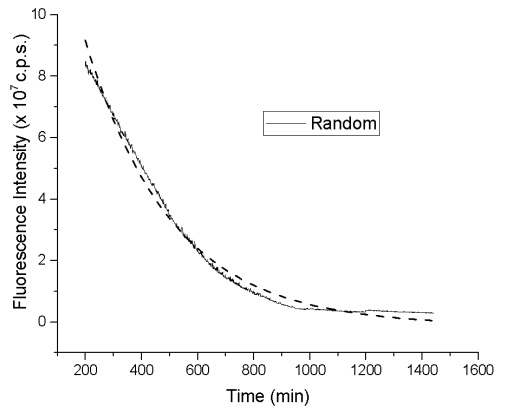


Figure S7: Effect of LED on the rate of DNA damage of different dsDNA targets

Table S1. Effect of different concentrations of LED and DAC on the damage induced in a random sequence of dsDNA.

Drug concentration (μM)	Damage constant “ τ ” (min)	
	LED	DAC
0.01	-----	1117 \pm 28.7 ($I_{F,0}$ =32.5 \pm 1.78 $\times 10^6$, A= 147 \pm 1.13 $\times 10^6$)
0.1	735 \pm 15.0 ($I_{F,0}$ =2.31 \pm 0.57 $\times 10^6$, A= 81.0 \pm 0.32 $\times 10^6$)	1255 \pm 32.8 ($I_{F,0}$ =38.1 \pm 0.99 $\times 10^6$, A= 150 \pm 1.42 $\times 10^6$)
1	827 \pm 5.24 ($I_{F,0}$ =8.88 \pm 0.18 $\times 10^6$, A= 75.8 \pm 0.10 $\times 10^6$)	1161 \pm 25.7 ($I_{F,0}$ =36.9 \pm 1.73 $\times 10^6$, A= 163 \pm 1.15 $\times 10^6$)
10	499 \pm 1.01 ($I_{F,0}$ =1.05 \pm 0.04 $\times 10^6$, A= 70.0 \pm 0.07 $\times 10^6$)	1082 \pm 17.1 ($I_{F,0}$ =95.7 \pm 2.63 $\times 10^6$, A= 393 \pm 1.22 $\times 10^6$)
20	490 \pm 6.68 ($I_{F,0}$ =6.73 \pm 0.37 $\times 10^6$, A= 123 \pm 0.75 $\times 10^6$)	1212 \pm 16.4 ($I_{F,0}$ =112 \pm 2.17 $\times 10^6$, A= 345 \pm 1.25 $\times 10^6$)

30	497± 7.63 ($I_{F,0}$ =6.05±0.40×10 ⁶ , A= 102±0.54×10 ⁶)	738± 6.48 ($I_{F,0}$ =45.8±0.93×10 ⁶ , A= 324±0.53×10 ⁶)
40	411±4.48 ($I_{F,0}$ =3.51±0.24×10 ⁶ , A= 129±0.88×10 ⁶)	525± 5.33 ($I_{F,0}$ =24.2±0.68×10 ⁶ , A= 312±1.52×10 ⁶)
60	345±2.76 ($I_{F,0}$ =0.55±0.01×10 ⁶ , A= 130±0.86×10 ⁶)	246± 1.91 ($I_{F,0}$ =4.54±0.28×10 ⁶ , A= 560±5.01×10 ⁶)
80	277± 1.96 ($I_{F,0}$ =0.03±0.01×10 ⁶ , A= 169±1.32×10 ⁶)	248± 1.80 ($I_{F,0}$ =4.57±0.25×10 ⁶ , A= 608±7.05×10 ⁶)
100	262± 1.73 ($I_{F,0}$ =0.79±0.01×10 ⁶ , A= 187±1.47×10 ⁶)	234± 1.95 ($I_{F,0}$ =3.99±0.28×10 ⁶ , A= 484±3.58×10 ⁶)

EvaGreen fluorescence curve fitting parameters are shown for the different concentrations of LED and DAC used in this work. The fluorescence is fit to a single exponential function ($I_F = I_{F,0} + Ae^{-t/\tau}$), where A (c.p.s.) is the amplitude, $I_{F,0}$ (c.p.s.) is the y offset (shown in the brackets), and τ is the damage constant obtained from fitting the experimental data points in Figure 5. The random sequence dsDNA concentration was 0.2 μ M.

Table S2. Effect of LED and DAC on different sequences of DNA.

DNA Sequences	Damage constant “ τ ” (min)	
	LED	DAC
Random	204±1.29 ($I_{F,0}$ =2.53±0.07×10 ⁶ , A= 181±1.52×10 ⁶)	173±1.33 ($I_{F,0}$ =3.9±0.10×10 ⁶ , A= 722±114.4×10 ⁶)
poly-TG	306± 2.17 ($I_{F,0}$ =1.14±0.16×10 ⁶ , A= 178±1.07×10 ⁶)	223± 1.46 ($I_{F,0}$ =2.89±0.18×10 ⁶ , A= 762±9.91×10 ⁶)
poly-TC	298± 2.21 ($I_{F,0}$ =0.15±0.01×10 ⁶ , A= 162±1.12×10 ⁶)	230± 1.33 ($I_{F,0}$ =0.60±0.10×10 ⁶ , A= 665±7.41×10 ⁶)
poly-T	357± 3.55 ($I_{F,0}$ =1.84±0.07×10 ⁶ , A= 43.6±0.29×10 ⁶)	297± 2.84 ($I_{F,0}$ =0.79±0.01×10 ⁶ , A= 62.6±0.26×10 ⁶)

EvaGreen fluorescence curve fitting parameters are shown for all the oligonucleotide sequences used in this work. The fluorescence is fit to a single exponential function ($I_F = I_{F,0} + Ae^{-t/\tau}$), where A (c.p.s.) is the amplitude, $I_{F,0}$ (c.p.s.) is the y offset (shown in the brackets), and τ is the damage constant obtained from fitting the experimental data points in Figure 6. The drug concentrations were 100 μM each and the dsDNA concentration was 0.2 μM .